Interplay between *d*-wave superconductivity and a bond-density wave in the one-band Hubbard model

J. P. L. Faye* and D. Sénéchal

Département de physique and Institut Quantique, Université de Sherbrooke, Sherbrooke, Québec, Canada J1K 2R1

(Received 8 December 2016; revised manuscript received 9 February 2017; published 14 March 2017)

It is now well established that superconducting cuprates support a charge-density-wave state in the so-called underdoped region of their phase diagram. We investigate the possibility of charge order in the square-lattice Hubbard model, both alone and in coexistence with *d*-wave superconductivity. The charge order has a period of 4 in one direction, is centered on bonds, and has a *d* form factor. We use the variational cluster approximation, an approach based on a rigorous variational principle that treats short-range correlations exactly, with two clusters of size 2×6 that together tile the infinite lattice and provide a nonbiased unit for a period-4 bond-density wave (BDW). We find that the BDW exists in a finite range of hole doping and increases in strength from $U = 5$ to $U = 8$. Its location and intensity depend strongly on the band dispersion. When probed simultaneously with *d*-wave superconductivity, the energy is sometimes lowered by the presence of both phases, depending on the interaction strength. Whenever they coexist, a pair-density wave (a modulation of superconducting pairing with the same period and form factor as the BDW) also exists.

DOI: 10.1103/PhysRevB.95.115127

I. INTRODUCTION

Charge order in underdoped superconducting cuprates has been observed by many techniques and in many compounds. Nuclear magnetic resonance measurements on $YBa_2Cu_3O_y$ indicate the presence of a long-range, static charge order without any signature of spin order [1,2]. In $Bi_2Sr_2CaCu_2O_{8+\delta}$, scanning tunneling microscopy (STM) shows a periodic modulation in the density of states [3,4]. Charge-density-wave correlations have also been observed in x-ray scattering [5–7], and the charge-density wave seems to be directed along copper oxygen bonds [8]. STM measurements also indicate that the charge-density-wave modulation resides on Cu-O-Cu bonds [4,9,10]. The dependence of the peak intensity as a function of magnetic field clearly indicates the possibility of a competition between *d*-wave superconductivity and charge-density-wave order [7]. More recently, the pair-density wave (PDW) that coexists with *d*-wave superconductivity and charge order has also been observed [11].

Theoretical investigations of charge order in cuprates roughly fall into two categories: (i) those that study the effect of static charge order on observables and (ii) those that attempt at explaining the origin of charge order from a model Hamiltonian with interactions. This work belongs to the second category. A few attempts have been made in that direction in the literature. For instance, Vojta [12] applied mean-field theory to the t-J model plus extended interactions and mapped out various charge-order phases that appear when J is low enough, whereas *d*-wave superconductivity dominates at higher J. A pure exchange model (without correlated hopping) has also been studied at the mean-field level by Sachdev and La Placa [13]. Atkinson *et al.* applied the generalized random-phase approximation to the full three-band Hubbard model [14] and view charge order, like the pseudogap, as a side effect of short-range antiferromagnetic correlations. The Gutzwiller approximation was applied to the Hubbard model (without extended interactions) but no charge order was found with that approach [15]. Renormalized mean-field theory (based on the Gutzwiller approximation) applied to the t-J model indicated that a large variety of nearly degenerate spin- and charge-order states may coexist with *d*-wave superconductivity [16,17]. Charge order at half filling in the extended Hubbard model was recently investigated with the dynamical cluster approximation [18], where it should be competition with antiferromagnetism. That competition was also studied in the context of the Hubbard-Holstein model [19], in which optical phonons would favor charge order over antiferromagnetism.

There is also a vast literature on stripe order, i.e., a coexistence of charge- and spin-density waves, which we do not review here. Let us mention nonetheless the work of Corboz *et al.* [20] in which the nearest-neighbor t-J model is studied using the projected-entangled pair states (PEPS) variational ansatz, and where stripe order occurs naturally in coexistence with *d*-wave superconductivity. This is consistent with the previous work of Capello *et al.* [21] on the same model using the variational Monte Carlo approach. Finally, the PDW state has been the focus of many studies [22–26] (for a recent review, see Ref. [27]).

In this work we investigate whether a particular charge-density-wave (CDW) order can arise from local repulsive interactions alone, and whether it can coexist with *d*-wave superconductivity. To this end, we apply the variational cluster approximation (VCA) [28–30] to the one-band repulsive Hubbard model. The charge-density wave studied is bond centered, has a *d*-wave form factor, and is henceforth referred to as a bond-density wave (BDW). The VCA, and other quantum cluster methods such as cluster dynamical mean-field theory [31,32] and the dynamical cluster approximation [33] already predict the presence of *d*-wave superconductivity in the doped one-band Hubbard model [34–36]. We find that a bond-density wave is indeed possible in the doped Hubbard model and that this phase is more robust when increasing the interaction strength U. Its location is also sensitive to the

*Present address: Abdus Salam International Center for Theoretical Physics, Strada Costiera 11, Trieste 34014, Italy.

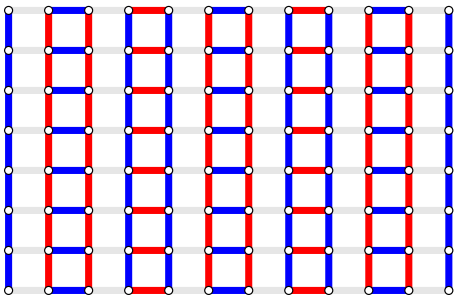

FIG. 1. Bond-density-wave pattern studied in this work. Blue means positive, red negative, and gray zero.

detailed band structure. In addition, we find that the BDW can coexist with d-wave superconductivity (dSC), although both the dSC and BDW order parameters are negatively affected by their coexistence. A PDW order also sets in when BDW and dSC orders coexist.

This paper is organized as follows: in Sec. II, we describe the particular BDW studied and briefly review the VCA method; in Sec. III, we present and discuss our numerical results. Finally, we conclude in Sec. IV.

II. MODEL AND METHOD

Let us first establish some notation. The one-band Hubbard model on a square lattice is defined by the following Hamiltonian:

$$H = -t \sum_{\langle \mathbf{r},\mathbf{r}'\rangle,\sigma} c^\dagger_{\mathbf{r},\sigma} c_{\mathbf{r}',\sigma} + U \sum_{\mathbf{r}} n_{\mathbf{r},\uparrow} n_{\mathbf{r},\downarrow} - \mu \sum_{\mathbf{r},\sigma} n_{\mathbf{r},\sigma}, \quad (1)$$

where $c_{\mathbf{r},\sigma}$ destroys an electron of spin σ at site $\mathbf{r}$ on the lattice; $n_{\mathbf{r},\sigma} = c^\dagger_{\mathbf{r},\sigma} c_{\mathbf{r},\sigma}$ is the number of electrons of spin σ at site $\mathbf{r}$. The chemical potential μ is included in the Hamiltonian for convenience.

Following Ref. [37], a general BDW operator of wave vector $\mathbf{q}$ is defined as follows:

$$\hat{\Psi}_{\mathrm{BDW}} = \sum_{\mathbf{r}\sigma,\mathbf{a}} t_{\mathbf{q},\mathbf{a}} c^\dagger_{\mathbf{r},\sigma} c_{\mathbf{r}+\mathbf{a},\sigma} e^{i(\mathbf{q}\cdot\mathbf{r}+\mathbf{a}/2)} + \mathrm{H.c.} \quad (2)$$

We probe a BDW of period 4, with d-wave form factor: $\mathbf{q} = (\pi/2,0)$, with $t_{\mathbf{q},\hat{\mathbf{y}}} = -t_{\mathbf{q},\hat{\mathbf{x}}} \equiv -1/\sqrt{2}$. The d-wave form factor is supported by STM observations [38]. The period 4 is also supported by STM data [3], but generally an inverse period somewhere between 0.25 and 0.3 is reported. This BDW is illustrated in Fig. 1. This choice is motivated by its simple commensurability and its compatibility with the cluster method we use, as explained below.

We also probe d-wave superconductivity, with a pair operator defined as

$$\hat{\Psi}_{\mathrm{dSC}} = \sum_{\mathbf{r},\mathbf{a}=\hat{\mathbf{x}},\hat{\mathbf{y}}} \Delta_{\mathbf{a}} (c_{\mathbf{r},\uparrow} c_{\mathbf{r}+\mathbf{a},\downarrow} - c_{\mathbf{r},\downarrow} c_{\mathbf{r}+\mathbf{a},\uparrow}) + \mathrm{H.c.}, \quad (3)$$

where $\Delta_{\hat{\mathbf{x}}} = 1$ and $\Delta_{\hat{\mathbf{y}}} = -1$. If both superconductivity and charge order are present, the pair-density wave (singlet) order parameter

$$\hat{\Psi}_{\mathrm{PDW}} = \sum_{\mathbf{r},\mathbf{a}} t_{\mathbf{q},\mathbf{a}} (c_{\mathbf{r},\uparrow} c_{\mathbf{r}+\mathbf{a},\downarrow} - c_{\mathbf{r},\downarrow} c_{\mathbf{r}+\mathbf{a},\uparrow}) e^{i(\mathbf{q}\cdot\mathbf{r}+\mathbf{a}/2)} + \mathrm{H.c.} \quad (4)$$

should also be nonzero.

The variational cluster approximation

In order to probe the possibility of superconductivity and bond-density wave as well as their coexistence in model (1), we use the VCA with an exact diagonalization solver at zero temperature [29]. This method, which goes beyond mean-field theory by keeping the correlated character of the model, has been applied to many strongly correlated systems in connection with various broken-symmetry phases, in particular d-wave superconductivity [34,39]. For a detailed review of the method, see Refs. [40,41].

In essence, the VCA is a variational method on the electron self-energy. It can probe various broken symmetries (or just the normal state) by exploring a space of self-energies that are the actual self-energies of model (1), but restricted on a small cluster of sites and augmented by Weiss fields that probe broken symmetries and other one-body terms. Once the optimal self-energy in that space is found, it is added to the noninteracting Green function for the full lattice and, from there, various observables may be computed.

Like other quantum cluster methods, VCA starts by a tiling of the lattice into an infinite number of (usually identical) clusters. In VCA, one considers two systems: the original system described by the Hamiltonian H, defined on the infinite lattice, and the *reference system*, governed by the Hamiltonian H', defined on the cluster only, with the same interaction part as H. Typically, H' will be a restriction of H to the cluster (i.e., with intercluster hopping removed), to which various Weiss fields may be added in order to probe broken symmetries. More generally, any one-body term can be added to H'. The size of the cluster should be small enough for the electron Green function to be computed numerically.

The optimal one-body part of H' is determined by a variational principle. More precisely, the electron self-energy $\mathbf{\Sigma}$ associated with H' is used as a variational self-energy, in order to construct the following Potthoff self-energy functional [42]:

$$\Omega[\mathbf{\Sigma}(\xi)] = \Omega'[\mathbf{\Sigma}(\xi)] + \mathrm{Tr}\ln[-\left(\mathbf{G}_0^{-1} - \mathbf{\Sigma}(\xi)\right)^{-1}] - \mathrm{Tr}\ln(-\mathbf{G}'(\xi)). \quad (5)$$

The quantities $\mathbf{G}'$ and $\mathbf{G}_0$ above are respectively the physical Green function of the cluster and the noninteracting Green function of the infinite lattice. The symbol ξ stands for a small collection of parameters that define the one-body part of H'. Tr is a functional trace, i.e., a sum over frequencies, momenta, and bands, and Ω' is the grand potential of the cluster, i.e., its ground-state energy, since the chemical potential μ is included in the Hamiltonian. $\mathbf{G}'(\omega)$ and Ω' are computed numerically via the Lanczos method at zero temperature.

The Potthoff functional $\Omega[\mathbf{\Sigma}(\xi)]$ in Eq. (5) is computed exactly, but on a restricted space of the self-energies $\mathbf{\Sigma}(\xi)$ that are the physical self-energies of the reference Hamiltonian H'. We use a standard optimization method (e.g., Newton-Raphson) in the space of parameters ξ to find the stationary value of $\Omega(\xi)$:

$$\frac{\partial \Omega(\xi)}{\partial \xi} = 0. \quad (6)$$

This represents the best possible value of the self-energy $\mathbf{\Sigma}$, which is used, together with the noninteracting Green function

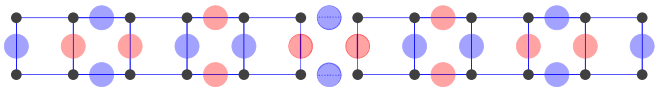

FIG. 2. The two 12-site clusters used in this work (black dots) with the BDW amplitudes (blue, positive; red, negative). These two clusters together form a unit that is repeated in both x and y directions. Note that changing the sign of the BDW amounts to interchanging the two clusters or to flipping each cluster about the vertical axis.

$\mathbf{G}_0$, to construct an approximate Green function $\mathbf{G}$ for the original lattice Hamiltonian H:

$$\mathbf{G}(\mathbf{k},\omega) = \frac{1}{\mathbf{G}_0^{-1}(\mathbf{k},\omega) - \mathbf{\Sigma}(\omega)}. \tag{7}$$

In the above the wave vector $\mathbf{k}$ is restricted to the reduced Brillouin zone associated with the superlattice defined by the cluster, and all boldface quantities are matrices of dimension L (or $2L$, if superconductivity is present), L being the number of sites in the cluster. From that Green function one can compute the average of any one-body operator, in particular order parameters associated with BDW or dSC.

The competition between orders can be studied by probing the two orders separately, and then together, in a coexistence scenario. If homogeneous coexistence is possible, then generally the associated value of Ω, which approximates the free energy in this approach, is lower than for the pure solutions for the two phases separately.

Charge-density waves, or other states that break translation symmetry, present a particular challenge to cluster methods like VCA, first because the unit cell of the density wave may be larger than the largest cluster that can be practically solved numerically, and second because cluster methods break translation symmetry from the outset. The first difficulty is solved by aggregating different clusters that together form a "supercluster" (or repeated unit) that tiles the lattice and that accommodates the charge-density wave. To overcome the second difficulty, one has to choose the clusters in such a way that the method is not biased towards the broken-symmetry state. In other words, if λ and Δ are the amplitudes of the Weiss fields associated with the BDW and dSC, respectively, then the Potthoff functional $\Omega(\lambda,\Delta)$ should be an even function of λ and Δ. Thus, the normal solution ($\lambda = \Delta = 0$) is always an option and the broken-symmetry state occurs if a nontrivial solution exists with a lower value of Ω. In this work, we use the two 12-site clusters shown in Fig. 2; the amplitudes of the bond charges in the particular BDW studied are indicated by colored circles. Together, these two clusters form a supercluster that contains three unit cells of the BDW. Changing the sign of the BDW amounts to flipping each cluster horizontally, which does not affect the value of $\Omega(\lambda,\Delta)$.

We give a few words on the computation of expectation values. The average of any one-body operator can be computed from the VCA solution in two different ways: (i) by taking its trace against the Green function or (ii) by differentiating the grand potential with respect to an external field. Let $s_{\alpha\beta}$ be the one-body matrix defining the operator $\hat{S}$, such that

$$\hat{S} = \sum_{\alpha,\beta} s_{\alpha\beta} c_\alpha^\dagger c_\beta \tag{8}$$

(α and β are compound indices, representing the site together with spin or other band indices). In a cluster approach, a partial Fourier transform can be applied to the site indices in $s_{\alpha\beta}$ to produce a reduced expression $s_{\alpha\beta}(\mathbf{k})$, where $\mathbf{k}$ belongs to the reduced Brillouin zone and the site indices are now limited to those of the repeated unit (the "supercluster"). In this language, the expectation value of $\hat{S}$ may be evaluated as

$$\langle \hat{S} \rangle = \int \frac{d\omega}{2\pi} \int_{\mathrm{rBZ}} \frac{d^2k}{(2\pi)^2} \mathrm{tr}[\mathbf{s}(\mathbf{k})\mathbf{G}(\omega,\mathbf{k})], \tag{9}$$

where the frequency integral is taken over a contour that circles the negative real axis, targeting the occupied states only. Alternatively, one may add an external field $s\hat{S}$ to the lattice Hamiltonian, compute the best estimate of the grand potential Ω for $s = 0$ and $s = \epsilon$ (i.e., the optimized self-energy functional), and compute the derivative

$$\langle \hat{S} \rangle = \frac{\partial \Omega}{\partial s} \approx \frac{\Omega(\epsilon) - \Omega(0)}{\epsilon}. \tag{10}$$

The two approaches (9) and (10) do not necessarily yield the same answer (the first one is less computationally intensive). In the case of a local operator, like the particle number $\hat{N}$, which does not contain intercluster components, it can be shown that the two approaches will yield the same value $n = \langle \hat{N} \rangle$ if the corresponding Weiss field on the cluster (in this case μ', the cluster's chemical potential) is treated as a variational parameter on the same level as the others (e.g., λ and Δ).

III. RESULTS AND DISCUSSION

In this section we report the results of VCA calculations on model (1) at various values of the interaction U and for a few band parameters. Since the simulations are somewhat time consuming, we could not explore the space of parameters *in extenso*, but our results illustrate how a bond-density wave can arise at finite doping in the presence of repulsive interactions, and in coexistence with d-wave superconductivity also arising from the same interaction.

A. Pure bond-density wave

We start by probing a pure BDW, without superconductivity. In VCA, this amounts to solving the following Hamiltonian on the cluster system of Fig. 2:

$$H' = H'_0 + \lambda \hat{\Psi}'_{\mathrm{BDW}}, \tag{11}$$

inserting the computed Green function into the expression (5) for the Potthoff functional, and finding the value of λ that minimizes the functional. In the above expression, H'_0 and $\hat{\Psi}'_{\mathrm{BDW}}$ are the restriction to the cluster of the kinetic energy operator and of the BDW operator (2), respectively. The coefficient λ was the only variational parameter used in optimizing the functional Ω. At this point, we have neglected the possible interaction with superconductivity. We comment on the interaction with antiferromagnetism towards the end of this section.

Figure 3(a) shows the optimal value of the Weiss field λ as a function of chemical potential μ, for a few values of the local repulsion U, and for second-neighbor hopping $t' = -0.3$ and third-neighbor hopping $t'' = 0$ and $t'' = 0.2$. Note that the

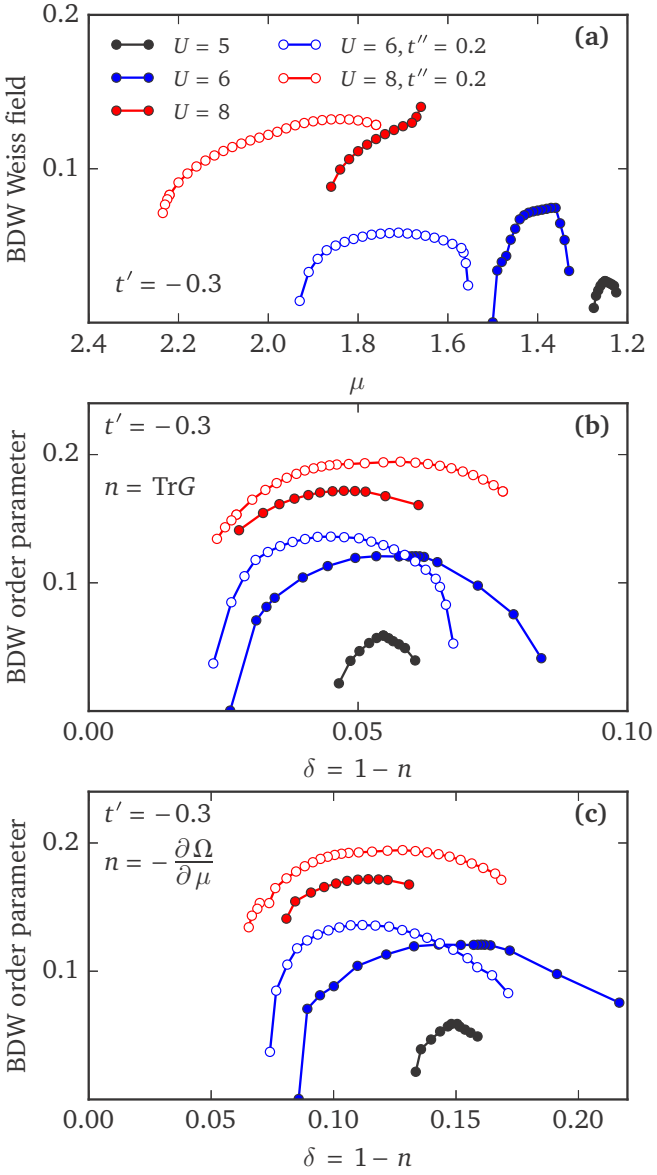

FIG. 3. (a) Optimal value of the Weiss field λ for the pure BDW phase as a function of chemical potential μ for various values of the interaction U and of the third-neighbor hopping t'', at $t' = -0.3$. The Weiss field goes generally to zero at the edge of the BDW phase, with the exception of $(U,t'') = (8,0.2)$. Note the direction of the axis: larger densities are on the left. (b) Corresponding BDW order parameter as a function of hole doping $\delta = 1 - n$ (n being the electron density), where n is computed from the Green function. (c) The same as in (b) except that the electron density is computed from the derivative of the grand potential Ω with respect to μ.

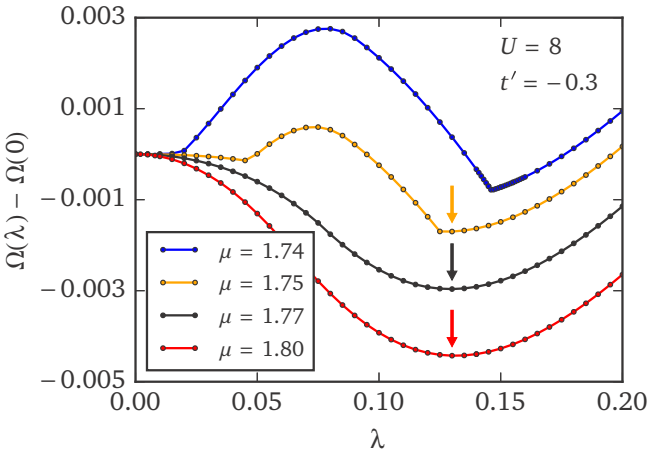

FIG. 4. Self-energy functional Ω as a function of Weiss field λ in the study of pure BDW. Acceptable VCA solutions are indicated by arrows. The data illustrate how the VCA solution may sometimes disappear because of the "intrusion" of segments with different behavior and the concomitant appearance of cusplike minima (top curve), which are not acceptable solutions.

nearest-neighbor hopping t is set to unity and thus defines the energy scale. These data constitute the "raw" solution from VCA. It is more physically instructive to look at the order parameter $\langle\hat{\Psi}_{\mathrm{BDW}}\rangle$ as a function of electron density n (or doping $\delta = 1 - n$), as is done in Figs. 3(b) and 3(c). We show the raw data in Fig. 3(a) in order to shed some light on the method itself.

Note that the transition from the BDW phase to the normal phase can proceed in many ways: (i) the Weiss field λ can go to zero at the phase boundary (continuous transition) or (ii) the solution can jump from a finite value of λ to zero, either because the solution becomes metastable at that point or because it ceases to exist (the derivative at the minimum is no longer defined, i.e., the functional Ω acquires a cusplike behavior). The latter type occurs in the figure for $(U,t'') = (8,0.2)$. Figure 4 illustrates this last point by showing plots of Ω(λ) for a few values of μ. We see how the smooth minimum (indicated by arrows) disappears at some value of μ as Ω(λ) acquires nondifferentiable features. This behavior is an occasional drawback of the method and is likely dependent on the shape and size of the cluster, on the type of Weiss field considered, etc. (We have checked that this behavior is not caused by a sudden change in the cluster ground state leading to a discontinuity in the cluster density.) In the continuous case the order parameter goes to zero smoothly, whereas it jumps discontinuously in the second case. A more conventional first-order transition, in which two distinct bona fide solutions have the same value of Ω at some value of an external parameter, is also possible but has not been observed here.

Figure 3(b) shows the BDW order parameter $\langle\hat{\Psi}_{\mathrm{BDW}}\rangle$ as a function of hole doping, both computed from the Green function [Eq. (9)], for the same data sets as those appearing in Fig. 3(a). Figure 3(c) shows the same data, this time with the density computed from the derivative of Ω with respect to μ. The values of doping obtained by these two approaches differ by roughly a factor of 2. Whatever the method of computing n, it appears that the BDW is increasing in strength with U and is also quite sensitive on the band dispersion; in particular, no BDW order occurs at $(U,t'') = (5,0.2)$.

An apparent way out of the ambiguity in the way to compute electron density is to treat the cluster chemical potential μ' as a variational parameter, on the same level as the Weiss field λ. When this is done, the data of Fig. 5 are obtained (this was done for $t' = -0.3$ and $t'' = 0$ only). Figure 5(a) shows the Weiss

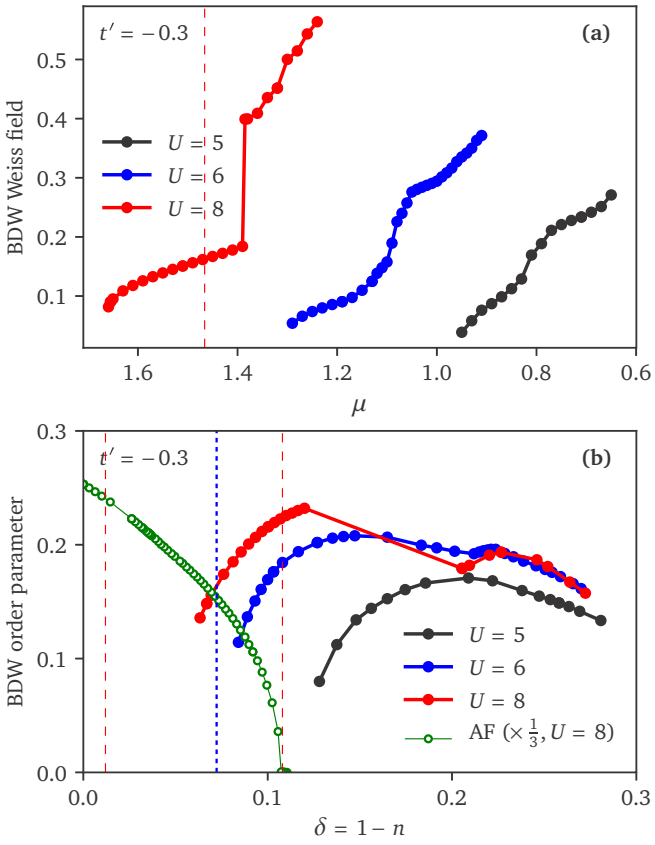

FIG. 5. (a) Optimal value of the Weiss field λ for the pure BDW phase as a function of chemical potential μ for various values of the interaction U and $t' = 0$, this time by treating the cluster chemical potential μ' as a variational parameter as well. The dashed vertical line indicates the chemical potential at which the free energy Ω of the BDW solution crosses that of the pure antiferromagnetic solution at $U = 8$ (the latter has a lower energy on the left of that line). (b) Corresponding BDW order parameter as a function of doping δ. This time, the two methods for computing the electron density are consistent with one another. The Green curve shows the competing pure antiferromagnetic (AF) order parameter at $U = 8$. The red dashed line of (a) corresponds to the two red dashed lines (two different dopings) shown here. The blue dotted line is the doping beyond which the energy $\Omega + \mu n$ of the BDW solution at $U = 8$ is lower than that of the AF solution.

field as a function of μ, and Fig. 5(b) shows the BDW order parameter as a function of doping. Note that the Weiss field tends to larger values on the overdoped side (smaller μ). This leads us to think that the overdoped results are less reliable: the "canonical" phase transition in VCA has the Weiss field go to zero at the same time as the order parameter. A discontinuity in the solution for $U = 8$, also mildly apparent at $U = 6$, reinforces this point of view.

We also show, in Fig. 5, a comparison, at $U = 8$, between pure antiferromagnetic (AF) and BDW solutions. The AF order parameter is shown in Fig. 5(b) (green curve). The free energies Ω of the two competing states cross at a value of the chemical potential μ indicated by a red dashed line in Fig. 5(a). This value of μ corresponds to two different values of the density (or doping) in the two solutions, indicated by red dashed lines in Fig. 5(b), and leaving a gap between them in which one could theoretically expect a macroscopic coexistence (phase separation) of the two states (ignoring the possibility of all other states, of course). On the other hand, it is also possible to compare the energies $E = \Omega + \mu n$ (n is the density) of the two states, and the blue dotted line in Fig. 5(b) indicates the doping beyond which the BDW state has a lower energy than the AF state. For lower values of U, the AF state will stay closer to half filling and the BDW states move away from half filling, thus reducing the competition between the two. We have not found any solution where the AF and BDW states are in homogeneous coexistence.

To conclude this part, model (1) indeed supports a pure bond-density wave as the particular one studied here, but the VCA is not too reliable as to the precise doping range where it occurs. The BDW appears quite sensitive to the dispersion relation, as expected. It appears beyond a certain threshold value of U and grows with U up to intermediate coupling. It is not preempted by antiferromagnetic order. Note that the d-wave form factor of the BDW is crucial. We have looked for BDWs with an extended s-wave form factor (which differs from the d-wave form factor only by the sign of the y bonds) and did not find any nonzero solution (the Potthoff functional has a minimum at a vanishing value of the Weiss field).

B. Bond-density wave and d-wave superconductivity

We now proceed to probe solutions in which dSC coexists with the BDW. This is done by adding both BDW and dSC terms, as defined by Eqs. (2) and (3), to the cluster Hamiltonian:

$$H' = H'_0 + \lambda \hat{\Psi}'_{\mathrm{BDW}} + \Delta \hat{\Psi}'_{\mathrm{dSC}}. \tag{12}$$

We start by studying the case with nearest-neighbor hopping only ($t' = t'' = 0$), for $U = 5$ and $u = 6$. Figure 6 shows the dSC and BDW order parameters both for the pure and the coexistence solutions as a function of the hole doping δ [the "pure" solutions are obtained by setting one of the Weiss fields (λ or Δ) to zero]. The electron density was computed from the Green function. The pure dSC solution exists in a large doping interval, with a maximum at $\delta = 10\%$. Antiferromagnetic order was not put in competition with dSC order, since we are focusing on the interplay between dSC and BDW. The striking effect shown here is that the interaction of the two phases tends to suppress superconductivity at $U = 6$, whereas it tends to suppress charge order at $U = 5$. The PDW order parameter is also shown (orange dots). In this work a PDW Weiss field was not used as a variational parameter. (That would have added to the complexity and length of the computations.) But whenever the BDW and dSC orders are both present, a nonzero PDW amplitude is inevitable; i.e., it is not forbidden by symmetry.

Figure 7 shows results obtained with a more realistic band dispersion ($t' = -0.3$), at $U = 8$. This time, the pure dSC solution always has a lower energy than the pure BDW solution, contrary to the solution found at $(U,t') = (6,0)$. Nevertheless, the coexistence solution has a lower energy than the pure dSC solution from $\delta \sim 9\%$ on. We do not believe the solutions beyond $\delta = 15\%$ (not shown) to be reliable, as they display the same type of discontinuity as shown in Fig. 5.

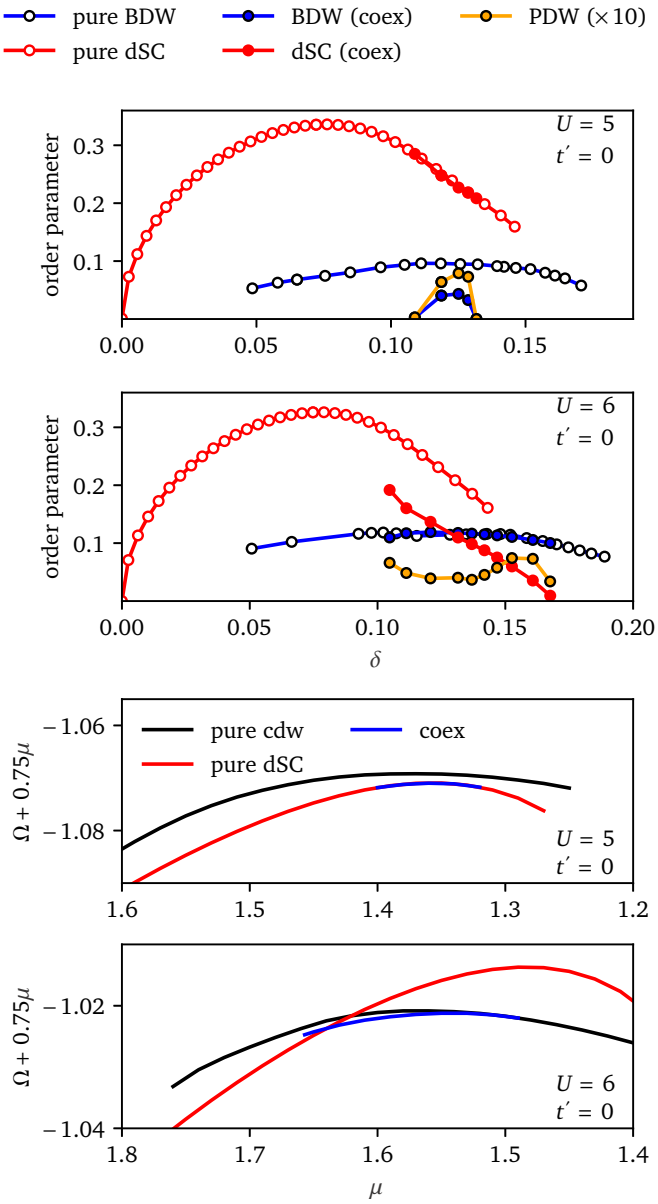

FIG. 6. dSC and BDW order parameters as a function of hole doping $\delta = 1 - n$ for $U = 5$ and $U = 6$ at $t' = t'' = 0$. The pair-density wave (PDW) order parameter $\langle \hat{\Psi}_{\mathrm{PDW}} \rangle$ is also shown (note the change of scale); the latter only exists in the coexistence phase. The bottom two panels show the free energies Ω of the same solutions (shifted by a multiple of μ in order to improve readability) as a function of the chemical potential.

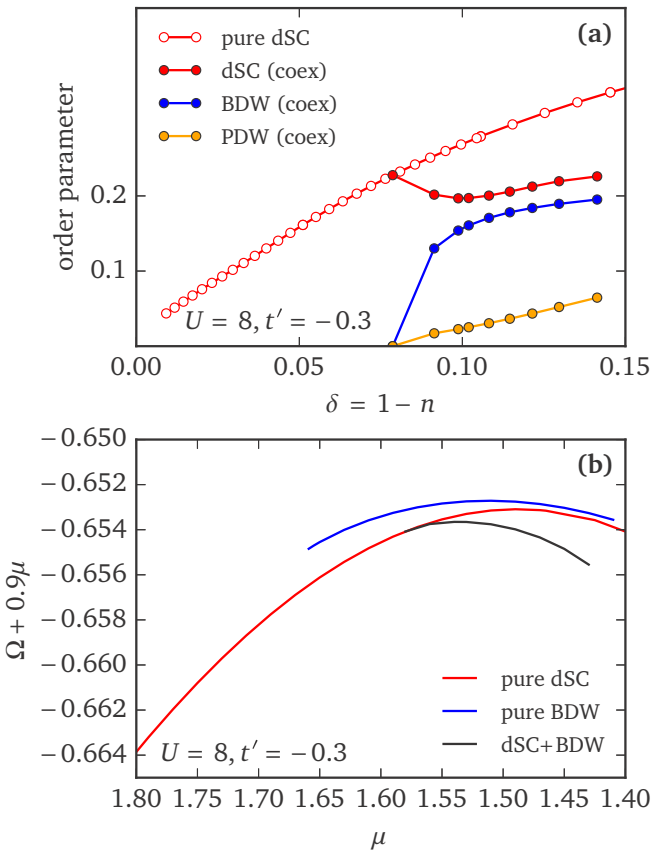

FIG. 7. (a) dSC, BDW, and PDW order parameters as a function of hole doping δ for $U = 8$ and $t' = -0.3$. The two orders were put in competition. The open red circles show the dSC order parameter when probed alone. In this data set the cluster chemical potential μ' was treated as a variational parameter, in addition to the Weiss fields Δ and λ. Note the dip in dSC order as the BDW order appears. (b) The free energy Ω of the three solutions, as a function of μ (note that the axis is reversed). The coexistence solution has the lowest energy but exists in a narrower range of doping. The pure dSC solution always has a lower energy than the pure BDW solution shown in Fig. 5.

Note that the dSC solution reconnects to the pure-dSC solution when the BDW falls to zero, at $\delta \sim 8\%$.

The VCA approach used in this work has strengths and weaknesses. The main strength is that the problem can be treated at all: In the context of the intermediate coupling, repulsive Hubbard model, VCA and other quantum cluster methods [cellular dynamical mean-field theory and dynamical cluster approximation) are among the few options capable of revealing d-wave superconductivity; the effective pairing interaction is dynamically generated within the clusters used. In addition, treating a period-4 BDW can be done elegantly with 2×6 clusters, which are too large to be treated with an exact diagonalization solver (hence at zero temperature) in any other approach than VCA. Seeing both BDW and dSC emerging from the same repulsive interaction, in coexistence, is particularly satisfying.

On the flip side, VCA, contrary to dynamical mean-field theory (DMFT)-like approaches, does not let particles in and out of the cluster (there are no bath degrees of freedom) and this leads to a less reliable estimate of the electron density. The approach is prone to (likely spurious) first-order phase transitions that occur when doping is pushed too far. In addition, the approach is numerically more delicate than DMFT and convergence may be more difficult. Finally, in practice, it can only probe orders that are defined from the outset (i.e., it is somewhat restricted).

IV. CONCLUSION

Figure 7 is the most significant result of this work. It shows how a particular bond-density wave and d-wave

superconductivity both emerge dynamically from the one-band Hubbard model and how they are intertwined in a finite range of hole doping, for a realistic dispersion relation.

In this work only local interactions are responsible for the establishment of both charge order and d-wave superconductivity. It is reasonable to expect that extended interactions will reinforce the tendency towards charge order; in the context of quantum cluster methods, extended interactions need to be treated partly in the Hartree approximation (the so-called dynamical Hartree approximation [43]). Work in that direction would be the natural next step.

ACKNOWLEDGMENTS

We thank A.-M. Tremblay for fruitful discussions. Computing resources were provided by Compute Canada and Calcul Québec. This research is supported by NSERC Grant No. RGPIN-2015-05598 (Canada) and by Fonds de recherche du Québec : nature et technologies (FRQNT) (Québec).

[1] T. Wu, H. Mayaffre, S. Krämer, M. Horvatić, C. Berthier, W. N. Hardy, R. Liang, D. A. Bonn, and M.-H. Julien, Magnetic-field-induced charge-stripe order in the high-temperature superconductor $YBa_2Cu_3O_y$, Nature (London) **477**, 191 (2011).

[2] T. Wu, H. Mayaffre, S. Krämer, M. Horvatić, C. Berthier, P. L. Kuhns, A. P. Reyes, R. Liang, W. N. Hardy, D. A. Bonn, and M.-H. Julien, Emergence of charge order from the vortex state of a high-temperature superconductor, Nat. Commun. **4**, 2113 (2013).

[3] J. E. Hoffman, E. W. Hudson, K. M. Lang, V. Madhavan, H. Eisaki, S. Uchida, and J. C. Davis, A four unit cell periodic pattern of quasi-particle states surrounding vortex cores in $Bi_2Sr_2CaCu_2O_{8+\delta}$, Science **295**, 466 (2002).

[4] M. Vershinin, S. Misra, S. Ono, Y. Abe, Y. Ando, and A. Yazdani, Local ordering in the pseudogap state of the high-T_c superconductor $Bi_2Sr_2CaCu_2O_{8+\delta}$, Science **303**, 1995 (2004).

[5] G. Ghiringhelli, M. Le Tacon, M. Minola, S. Blanco-Canosa, C. Mazzoli, N. B. Brookes, G. M. De Luca, A. Frano, D. G. Hawthorn, F. He, T. Loew, M. Moretti Sala, D. C. Peets, M. Salluzzo, E. Schierle, R. Sutarto, G. A. Sawatzky, E. Weschke, B. Keimer, and L. Braicovich, Long-range incommensurate charge fluctuations in $(Y,Nd)Ba_2Cu_3O_{6+x}$, Science **337**, 821 (2012).

[6] A. J. Achkar, R. Sutarto, X. Mao, F. He, A. Frano, S. Blanco-Canosa, M. Le Tacon, G. Ghiringhelli, L. Braicovich, M. Minola, M. Moretti Sala, C. Mazzoli, R. Liang, D. A. Bonn, W. N. Hardy, B. Keimer, G. A. Sawatzky, and D. G. Hawthorn, Distinct Charge Orders in the Planes and Chains of Ortho-III-Ordered $YBa_2Cu_3O_{6+\delta}$ Superconductors Identified by Resonant Elastic X-Ray Scattering, Phys. Rev. Lett. **109**, 167001 (2012).

[7] J. Chang, E. Blackburn, A. T. Holmes, N. B. Christensen, J. Larsen, J. Mesot, Ruixing Liang, D. A. Bonn, W. N. Hardy, A. Watenphul, M. v. Zimmermann, E. M. Forgan, and S. M. Hayden, Direct observation of competition between superconductivity and charge density wave order in $YBa_2Cu_3O_{6.67}$, Nat. Phys. **8**, 871 (2012).

[8] E. Blackburn, J. Chang, M. Hücker, A. T. Holmes, N. B. Christensen, R. Liang, D. A. Bonn, W. N. Hardy, U. Rütt, O. Gutowski, M. v. Zimmermann, E. M. Forgan, and S. M. Hayden, X-Ray Diffraction Observations of a Charge-Density-Wave Order in Superconducting Ortho-II $YBa_2Cu_3O_{6.54}$ Single Crystals in Zero Magnetic Field, Phys. Rev. Lett. **110**, 137004 (2013).

[9] Y. Kohsaka, C. Taylor, K. Fujita, A. Schmidt, C. Lupien, T. Hanaguri, M. Azuma, M. Takano, H. Eisaki, H. Takagi, S. Uchida, and J. C. Davis, An intrinsic bond-centered electronic glass with unidirectional domains in underdoped cuprates, Science **315**, 1380 (2007).

[10] A. J. Achkar, F. He, R. Sutarto, J. Geck, H. Zhang, Y.-J. Kim, and D. G. Hawthorn, Resonant X-Ray Scattering Measurements of a Spatial Modulation of the Cu $3d$ and O $2p$ Energies in Stripe-Ordered Cuprate Superconductors, Phys. Rev. Lett. **110**, 017001 (2013).

[11] M. H. Hamidian, S. D. Edkins, S. H. Joo, A. Kostin, H. Eisaki, S. Uchida, M. J. Lawler, E.-A. Kim, A. P. Mackenzie, K. Fujita, J. Lee, and J. C. Séamus Davis, Detection of a Cooper-pair density wave in $Bi_2Sr_2CaCu_2O_{8+x}$, Nature (London) **532**, 343 (2016).

[12] M. Vojta, Superconducting charge-ordered states in cuprates, Phys. Rev. B **66**, 104505 (2002).

[13] S. Sachdev and R. L. Placa, Bond Order in Two-Dimensional Metals with Antiferromagnetic Exchange Interactions, Phys. Rev. Lett. **111**, 027202 (2013).

[14] W. A. Atkinson, A. P. Kampf, and S. Bulut, Charge order in the pseudogap phase of cuprate superconductors, New J. Phys. **17**, 013025 (2015).

[15] R. S. Markiewicz, J. Lorenzana, G. Seibold, and A. Bansil, Competing phases in the cuprates: Charge vs spin order, J. Phys. Chem. Solids **72**, 333 (2011).

[16] K.-Y. Yang, W. Q. Chen, T. M. Rice, M. Sigrist, and F.-C. Zhang, Nature of stripes in the generalized t-J model applied to the cuprate superconductors, New J. Phys. **11**, 055053 (2009).

[17] W.-L. Tu and T.-K. Lee, Genesis of charge orders in high temperature superconductors, Sci. Rep. **6**, 18675 (2016).

[18] H. Terletska, T. Chen, and E. Gull, Charge ordering and correlation effects in the extended Hubbard model, arXiv:1611.07861.

[19] J. Bauer and A. C. Hewson, Competition between antiferromagnetic and charge order in the Hubbard-Holstein model, Phys. Rev. B **81**, 235113 (2010).

[20] P. Corboz, S. R. White, G. Vidal, and M. Troyer, Stripes in the two-dimensional t-J model with infinite projected entangled-pair states, Phys. Rev. B **84**, 041108(R) (2011).

[21] M. Capello, M. Raczkowski, and D. Poilblanc, Stability of RVB hole stripes in high-temperature superconductors, Phys. Rev. B **77**, 224502 (2008).

[22] A. Himeda, T. Kato, and M. Ogata, Stripe States with Spatially Oscillating d-Wave Superconductivity in the Two-Dimensional t–t'–J Model, Phys. Rev. Lett. **88**, 117001 (2002).

[23] M. Raczkowski, M. Capello, D. Poilblanc, R. Frésard, and A. M. Oleś, Unidirectional d-wave superconducting domains in the two-dimensional t-J model, Phys. Rev. B **76**, 140505 (2007).

[24] P. Choubey, W.-L. Tu, T.-K. Lee, and P. J. Hirschfeld, Incommensurate charge ordered states in the t-t'-J model, New J. Phys. **19**, 013028 (2017).

[25] H. Freire, V. S. de Carvalho, and C. Pépin, Renormalization group analysis of the pair-density-wave and charge order within the fermionic hot-spot model for cuprate superconductors, Phys. Rev. B **92**, 045132 (2015).

[26] Y. Wang, D. F. Agterberg, and A. Chubukov, Coexistence of Charge-Density-Wave and Pair-Density-Wave Orders in Underdoped Cuprates, Phys. Rev. Lett. **114**, 197001 (2015).

[27] E. Fradkin, S. A. Kivelson, and J. M. Tranquada, Colloquium: Theory of intertwined orders in high temperature superconductors, Rev. Mod. Phys. **87**, 457 (2015).

[28] M. Potthoff, M. Aichhorn, and C. Dahnken, Variational Cluster Approach to Correlated Electron Systems in Low Dimensions, Phys. Rev. Lett. **91**, 206402 (2003).

[29] C. Dahnken, M. Aichhorn, W. Hanke, E. Arrigoni, and M. Potthoff, Variational cluster approach to spontaneous symmetry breaking: The itinerant antiferromagnet in two dimensions, Phys. Rev. B **70**, 245110 (2004).

[30] M. Aichhorn, H. G. Evertz, W. Von Der Linden, and M. Potthoff, Charge ordering in extended Hubbard models: Variational cluster approach, Phys. Rev. B **70**, 235107 (2004).

[31] A. I. Lichtenstein and M. I. Katsnelson, Antiferromagnetism and d-wave superconductivity in cuprates: A cluster dynamical mean-field theory, Phys. Rev. B **62**, R9283(R) (2000).

[32] G. Kotliar, S. Y. Savrasov, G. Pálsson, and G. Biroli, Cellular Dynamical Mean Field Approach to Strongly Correlated Systems, Phys. Rev. Lett. **87**, 186401 (2001).

[33] Th. Maier, M. Jarrell, Th. Pruschke, and J. Keller, d-Wave Superconductivity in the Hubbard Model, Phys. Rev. Lett. **85**, 1524 (2000).

[34] D. Sénéchal, P.-L. Lavertu, M.-A. Marois, and A.-M. S. Tremblay, Competition Between Antiferromagnetism and Superconductivity in High-T_c Cuprates, Phys. Rev. Lett. **94**, 156404 (2005).

[35] Th. Maier, M. Jarrell, T. C. Schulthess, P. R. C. Kent, and J. B. White, Systematic Study of d-Wave Superconductivity in the 2D Repulsive Hubbard Model, Phys. Rev. Lett. **95**, 237001 (2005).

[36] S. S. Kancharla, B. Kyung, D. Sénéchal, M. Civelli, M. Capone, G. Kotliar, and A.-M. S. Tremblay, Anomalous superconductivity and its competition with antiferromagnetism in doped Mott insulators, Phys. Rev. B **77**, 184516 (2008).

[37] A. Allais, D. Chowdhury, and S. Sachdev, Connecting high-field quantum oscillations to zero-field electron spectral functions in the underdoped cuprates, Nat. Commun. **5**, 5771 (2014).

[38] K. Fujita, M. H. Hamidian, S. D. Edkins, C. K. Kim, Y. Kohsaka, M. Azuma, M. Takano, H. Takagi, H. Eisaki, S.-I. Uchida, A. Allais, M. J. Lawler, E.-A. Kim, S. Sachdev, and J. C. S. Davis, Direct phase-sensitive identification of a d-form factor density wave in underdoped cuprates, Proc. Natl. Acad. Sci. USA **111**, E3026 (2014).

[39] M. Aichhorn, E. Arrigoni, M. Potthoff, and W. Hanke, Phase separation and competition of superconductivity and magnetism in the two-dimensional Hubbard model: From strong to weak coupling, Phys. Rev. B **76**, 224509 (2007).

[40] M. Potthoff, Self-energy-functional theory, in *Strongly Correlated Systems: Theoretical Methods*, Springer Series in Solid-State Sciences Vol. 171, edited by A. Avella and F. Mancini (Springer, New York, 2012), Chap. 9.

[41] M. Potthoff, Variational cluster approximation, in *DMFT at 25. Infinite Dimensions*, Lecture notes of the Autumn school on correlated electrons 2014, edited by E. Pavarini, E. Koch, D. Vollhardt, and A. Lichtenstein (Forschungszentrum, Jülich, 2014).

[42] M. Potthoff, Self-energy-functional approach to systems of correlated electrons, Eur. Phys. J. B **32**, 429 (2003).

[43] J. P. L. Faye, P. Sahebsara, and D. Sénéchal, Chiral triplet superconductivity on the graphene lattice, Phys. Rev. B **92**, 085121 (2015).